www.czasopisma.pan.pl PAN POLSKA AKADEMIA NAUK www.journals.pan.pl

Arch. Metall. Mater. **64** (2019), 1, 71-78

DOI: 10.24425/amm.2019.126220

M. BARTOSIEWICZ*#, A. CWUDZIŃSKI*

INFLUENCE OF MULTI-HOLE FILTER MODIFICATION ON THE FLOW HYDRODYNAMIC STRUCTURE AND REFINING PROCESS OF LIQUID STEEL IN THE ONE-STRAND TUNDISH

In this work, the authors proposed a modification of the working space one-strand tundish adapted for slab casting process. Numerical simulations of liquid steel flow in the considered flow reactor were performed. The tundish is equipped with a dam with a multi-hole filter. Two variants of the filter hole arrangement were tested and their effect on the liquid steel flow hydrodynamic structure in the tundish was examined. The computer calculations results were verified by performing experiments on the water model. The result of numerical and physical simulations an RTD (Residence Time Distribution) type F curve was generated, which define the transition zone between the cast steel grades during the sequential casting process. The results of the researches showed that the modification of a dam with a multi-hole filter affects on the formation of the liquid steel flow hydrodynamic structure and the transition zone. Furthermore, examinations of the liquid steel refining ability in the considered tundish were carried out. The influence of the filter holes arrangement on the non-metallic inclusions flotation process to the slag phase and liquid steel filtration processes was checked. Numerical simulations were performed in the Ansys-Fluent computer program.

Keywords: tundish, continuous steel casting, multi-hole filter, liquid steel flow, non-metallic inclusions

1. Introduction

An indispensable device of the continuous steel casting process is tundish, which the origin role is the ensuring continuous supply of liquid steel from steel ladle to the casting mold in the considered process. However, due to the increasing quality requirements of bloom, billets or slabs, the residence time of liquid steel in the tundish was used to perform treatments improving the purity level of liquid steel. A commonly used procedure to improve the tundish working conditions is interference in its working space through using flow control devices (FCD), which influences on the directions of liquid steel flow stream, modifying the hydrodynamic structure [1-4]. The considered treatments may improve the thermal and chemical homogenization of liquid steel. Also, it improves the generation of liquid steel active flow in the tundish and which can short the transition zone during mixing two cast steel grades in the sequential casting process (through the right ratio between plug and mixing flow). The turbulence inhibitors in a two-strand tundish were tested by T. Merder [5] and it was found that the use of FCD caused decreasing of the transition zone and increasing of active flow volume in the tundish. Also, the turbulence inhibitor and baffles in a two-strand tundish were researched by J. Pieprzyca et al. [6] and such as previous investigation, the modification of tundish working space by using FCD influence on the transition zone and active flow generation. Furthermore, the residence time of the liquid steel in the tundish can be used to refine it by removing non-metallic inclusions. The flotation process of non-metallic inclusions to the slag phase can be intensified through directing the liquid steel flow streams towards the upper surface of the metal in the tundish. Non-metallic inclusions distribution and separation in the one-strand tundish using impact pad were tested by A. Ruckert et al. [7]. It was found that used FCD in the tundish improves separation process of non-metallic inclusions in the slag phase. To increase the ability of the tundish to clean liquid steel from non-metallic inclusions, multi-hole filters are used. The filtration process is possible by contacting non-metallic inclusions with the filter wall. Some of the non-metallic inclusions flow through the filter, while other of the non-metallic inclusions adhere to the filter surface due to adsorption process, which was described in work [8]. Tests of liquid steel filtration process in tundish were performed in works [9-15]. In all tested cases, the use of a filter in a tundish caused a reduction in the content of non-metallic inclusions in the liquid steel. Methodology indicated in work [11] is helpful to designing a filter in a tundish by which finally it is possible to determine the coefficient of filtration area per unit of filtered steel mass, which is presented below:

$$W_F = \frac{P_F}{M_S} \tag{1}$$

where: W_F – filtration coefficient ($m^2 \cdot Mg^{-1}$); P_F – filtration area (m^2); M_S – mass of filtered steel (Mg).

* CZĘSTOCHOWA UNIVERSITY OF TECHNOLOGY, FACULTY OF PRODUCTION ENGINEERING AND MATERIALS TECHNOLOGY, DEPARTMENT OF METALS EXTRACTION AND RECIRCULATION, 19 ARMII KRAJOWEJ AVE, 42-200 CZĘSTOCHOWA, POLAND

Corresponding author: bartosiewicz.michal@wip.pcz.pl

Furthermore, dam with filter holes can be integrated with another FCD, what was presented in works [14,15]. The integration of two dams (which generate reaction chamber) with filter holes and bottom argon lance can provide the reduction of non-metallic inclusions in liquid steel by 2-2.5 times related to tundish without FCD. Also, filter holes can change the direction of the main liquid steel flow, what was shown in work [16]. In the tundish multi-hole filter with zigzag channels was adopted, which definitely change fields of liquid steel flow, turbulent kinetic energy and trajectories of non-metallic inclusions particles.

The search for the right solutions improving the tundish operations due to the problems of performing researches in industrial conditions, such as high costs of tests, high temperature of liquid steel, continuity of the casting process etc. is preceded by numerous and laboratory tests. Furthermore, liquid steel is covered by slag phase, which cause problems with assessment of the hydrodynamic structure in the tundish. Therefore, numerical simulations of liquid steel flow in the tundish are used [17-20]. However, the used mathematical model in the calculations and results of numerical simulations should be verified by performing laboratory experiments using a water model of tundish [21-24]. The supported numerical simulations results by the results from water modeling constitute important information for the implementation of innovative solutions in industrial conditions. Therefore, numerical simulations and water modeling were performed in this work. Authors proposed two multi-hole filters, which were installed in the tundish. Influence on the liquid steel flow hydrodynamic structure and affect on the refining processes were checked in the considered tundish.

2. Features of examined object

The research object is one-strand tundish, which in the continuous slab casting process is used. A nominal capacity of considered object is 30 Mg. Liquid steel via ladle shroud to the tundish is supplied, which on a depth 0.1 m in metal is submerged (ladle shroud internal diameter: 0.07 m). The object has two levels of the bottom through lowering the bottom in outlet zone of tundish. Continuous inflow of liquid steel to the casting mold via submerged entry nozzle is realized (liquid steel flow to the casting mold is controlled by stopper rod system). The considered tundish in a low dam with two overflow windows in front of the object outlet zone is equipped (in front of bottom lowering). The purpose of this device is suppression of liquid steel wave during the start of the casting process. The tundish working space expands in the direction of submerged entry nozzle. Detailed dimensions of the object are described in the work [25]. The idea of this article was checking the influence of the holes arrangement in the filter on the liquid steel hydrodynamic structure in the considered tundish. Two cases of multi-hole filter were performed, which in the tundish at the distance of 0.93 m from the axis of the ladle shroud were installed. In both cases the filter was enough high that the liquid steel flow was only carried out through the filter holes. Fig. 1 presents tundish virtual model with multi-hole filter (case 1) and two proposed research cases. The features of the considered multi-hole filters are summarized in table 1. The equation 1 was used to calculate of filtration coefficient (100 Mg of filtered steel mass was assumed).

TABLE 1

Features of the multi-hole filter cases

	Case 1	Case 2
Quantity of holes	21	
Thickness of filter [m]	0.15	
Diameter of holes [m]	0.0625	
Quantity of hole rows	3	
Distance between holes [m]	0.1	
Distance to first holes row from tundish bottom [m]	0.1	0.3
Filtration area of one hole [m^2]	0.0294	
Filtration coefficient [$m^2 \cdot Mg^{-1}$]	0.0062	

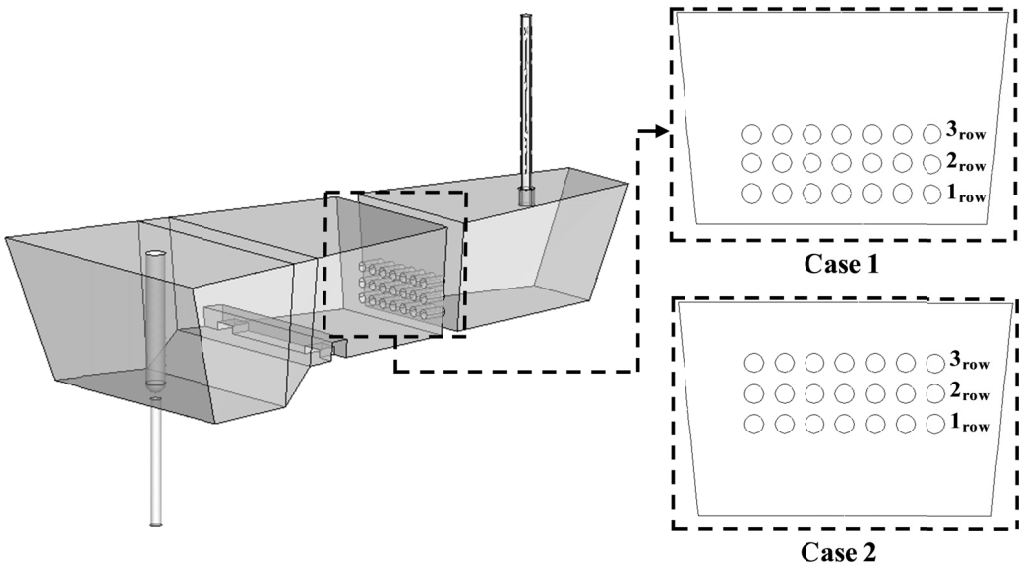

Fig. 1. Virtual model of the tundish with the considered research cases

3. Research methodology

The research range was consisted of three stages. The first stage was related to the numerical simulations of liquid steel flow in the considered tundish in isothermal conditions. The second stage concerned the performance of laboratory tests on a water model of a considered tundish equipped with a multi-hole filter. At this stage of research the mathematical model which were used in calculation was verified. The third stage was connected with the performance of liquid steel flow numerical simulations in non-isothermal conditions.

3D objects of a tundish with multi-hole filter in the Gambit computer program using the "bottom-up" and Boolean method to generate a virtual research object were performed. Then, tundish was descretized by a computational grid. Case 1 was divided to 278000, whereas case 2 to 276000 of the control elements. Finished tundish virtual models were imported through Ansys-Fluent computer program, in which the liquid steel flow numerical simulations of considered tundish were realized. Liquid steel flow was calculated using a mathematical model, which were described in detail in work [26]. The turbulent nature of the liquid steel flow taken into account in computer simulation, using a Realizable k-ε turbulence model, which widely described in works [27,28]. Mentioned turbulence model was tested in work [29] by comparing results from numerical simulation with water modeling. Verification outcomes indicate that the use in computer calculations the Realizable k-ε turbulence model correlates well with results from water modeling. Nevertheless, the verification of the mathematical model used in the calculations was again performed in this work, due to the changed tundish geometry by the installation of a multi-hole filter. The continuous steel casting process was simulated, casting a slab characterized by dimensions 1.5 × 0.225 m. Casting process with velocity of 0.015 $m \cdot s^{-1}$ was realized. Liquid steel through ladle shroud was flowed to the tundish. Therefore, boundary condition of flow location in the considered object established at the beginning of ladle shroud. Thanks to that the liquid steel flow hydrodynamic structure was simulated in entire volume of ladle shroud. Therefore, at the ladle shroud beginning the parameters of flowed liquid steel was established: velocity 1.316 $m \cdot s^{-1}$, turbulent kinetic energy 0.0173 $m^2 \cdot s^{-2}$, turbulent dissipation rate of kinetic energy 0.06514 $m^{-2} \cdot s^{-3}$ and temperature 1823 K (simulations in non-isothermal conditions). The equations of turbulent kinetic energy and turbulent dissipation rate were described in work [30]. Also, the physicochemical properties of liquid steel were used, such as: viscosity 0.007 $kg \cdot m^{-1} \cdot s^{-1}$, thermal conductivity 41 $W \cdot m^{-1} \cdot K^{-1}$, heat capacity 750 $J \cdot kg^{-1} \cdot K^{-1}$ (thermal conductivity and heat capacity in simulations in non-isothermal conditions were used). The liquid steel density in calculations in isothermal conditions was a constant, which was equal 7010 $kg \cdot m^{-3}$. In numerical simulations in non-isothermal conditions to calculate the liquid steel density a polynomial of temperature was used, which are presented in work [29]. The upper surface of the tested object imitated a boundary between liquid steel and slag. Furthermore, in computer simulations in non-isothermal conditions heat losses on the individual walls of the tundish taken into account, which are described in work [29]. The method of control elements integration through the second order discretization method was used in the mathematical model. The Semi-Implicit Method for Pressure-Linked Equations-Consistent (SIMPLEC) algorithm was used to describe the coupling of velocity and pressure fields. Furthermore, to solve the marker flow in the working space of the tundish the User Defined Scalar (UDS) transport equation was used. The results of numerical simulations of liquid steel flow in the considered tundish was the generation of an F-type RTD (Residence Time Distribution) curve, which is used to the assessment of mixing moment in the tundish of two casted successively steel grades, during sequential casting process (which is defined as the transition zone). The generation of F curve was performed through entering (continuous signal) the marker at the ladle shroud beginning and recording its concentration in submerged entry nozzle (at the exit of the tundish). Time and concentration in the F-type curve were converted into dimensionless values using the equations, which are described in works [25].

Shape of generated F curve from numerical simulations in isothermal conditions with results from laboratory experiments was verified , which on a physical model of tundish were performed. Thanks to that, it was possible to check mathematical model used in computer calculations. A physical model of tundish is constructed of glass, on a 2:5 scale (a similar scale of water model was used in another works [31,32]), which has a nominal capacity of 210 L [33]. The hydraulic system and flow meter are used to control the liquid flow in the physical model. While laboratory experiments the liquid that was simulating liquid steel was water, because it has the similar kinematic viscosity at 20°C, as a liquid steel at 1600°C. During performing the experiments in the tundish water model, the similarity terms between physical model and tundish used in industrial conditions were fulfilled. The Froude criterion is the most important criterion in the considered object, which ensures similarity of gravitational and inertia forces between water model and tundish used in industrial conditions [32,34]. The execution of the F curve on the water model depends on control of the water salinity change at the outflow of the considered object. To the water a marker in the form of KCl was added (potassium chloride). Thanks to that, the solution flowing through the simulator was characterized by higher salinity than "clean" water. The transition zone was simulated through supplying water to the physical model (through which water flows with dissolved KCl). The change in the salinity concentration of water at the outflow of water model was recording (in submerged entry nozzle) by a conductometric sensor. Measurements were performed every 10 s. Each laboratory experiments was repeated 6 times for individual case. Obtained measuring points were converting into dimensionless values. Then, its applied to F curves from numerical simulations in isothermal conditions and the comparing analysis of the transition zone shaping was performed. The transition zone can be modified due to type of cast slab [35,36]. For used casting conditions in this article the transition zone is determined in the range from 0.2 to 0.8 of the dimensionless concentration, which were verified in work [25].

Additionally, analysis of marker behavior in the tundish water model was performed. This analysis consisted of a color in the form of $KMnO_4$ marker the water flowing into the model. The marker spreading behind multi-hole filter in the individual cases were recorded by camera.

The results of numerical simulations in non-isothermal conditions of liquid steel flow was performed for the analysis of hydrodynamic structure and removing ability the non-metallic inclusions from liquid steel in the considered tundish. The Discrete Phase Model (DPM) was used to describe behavior of non-metallic inclusion particles [37]. Whereas, the Discrete Random Walk model (DRW) was used to simulate the chaotic movement of non-metallic inclusion particles in the tundish working space. In the computer calculations were established that non-metallic inclusion particles which reached boundary between liquid steel and slag from liquid steel were removed. A similar relationship was established, when the non-metallic inclusion particles reached the filter wall (internal surface in the individual holes of multi-hole filter). It should be noted that this can overstate the results of the removed non-metallic inclusion particles from liquid steel. Due to the fact that the tundish refining process is not only determined by the liquid steel flow hydrodynamic structure, but also thermodynamics and physico-chemical properties slag phase, non-metallic inclusions and filter refractory. Therefore, boundary condition for DPM model can be modified for improving the obtained results, what was determined in work [38]. However, obtained results using standard trap model can indicate the valuable information about refining process in the considered tundish. Al_2O_3 spherical particles as non-metallic inclusions were tested, which were characterized by the following properties: density 3960 $kg \cdot m^{-3}$, heat capacity 1364 $J \cdot kg^{-1} \cdot K^{-1}$. Non-metallic inclusion particles were added at the beginning of ladle shroud with main supplying stream of liquid steel in group of 5000 particles. 10 sizes of non-metallic inclusions were tested (in the range from 5 to 50 mm of particle diameter). The difference between individual particles was equal 5 mm. The analysis of the refining process in the considered tundish was made by recording (trajectories of each particle were followed in numerical simulations) the removed Al_2O_3 particles from liquid steel (to the slag phase and individual filter holes) and not removed Al_2O_3 particles which flow into the casting mold.

4. Research results

4.1. Behavior of marker in the tundish water model

Analysis of marker behavior during laboratory experiments on the tundish water model was performed. Tundish space behind multi-holes filter was taken into account to assess the main liquid steel streams in the considered object. Three photos from the recorded video were selected by comparing the spreading of the marker for both research cases after 5, 15 and 25 seconds from the moment, when the marker was entered into the water model (Fig. 2). Comparing fig. 2a with 2d, it can be seen that in case 2 slightly quicker the marker is appearing behind the multi-hole

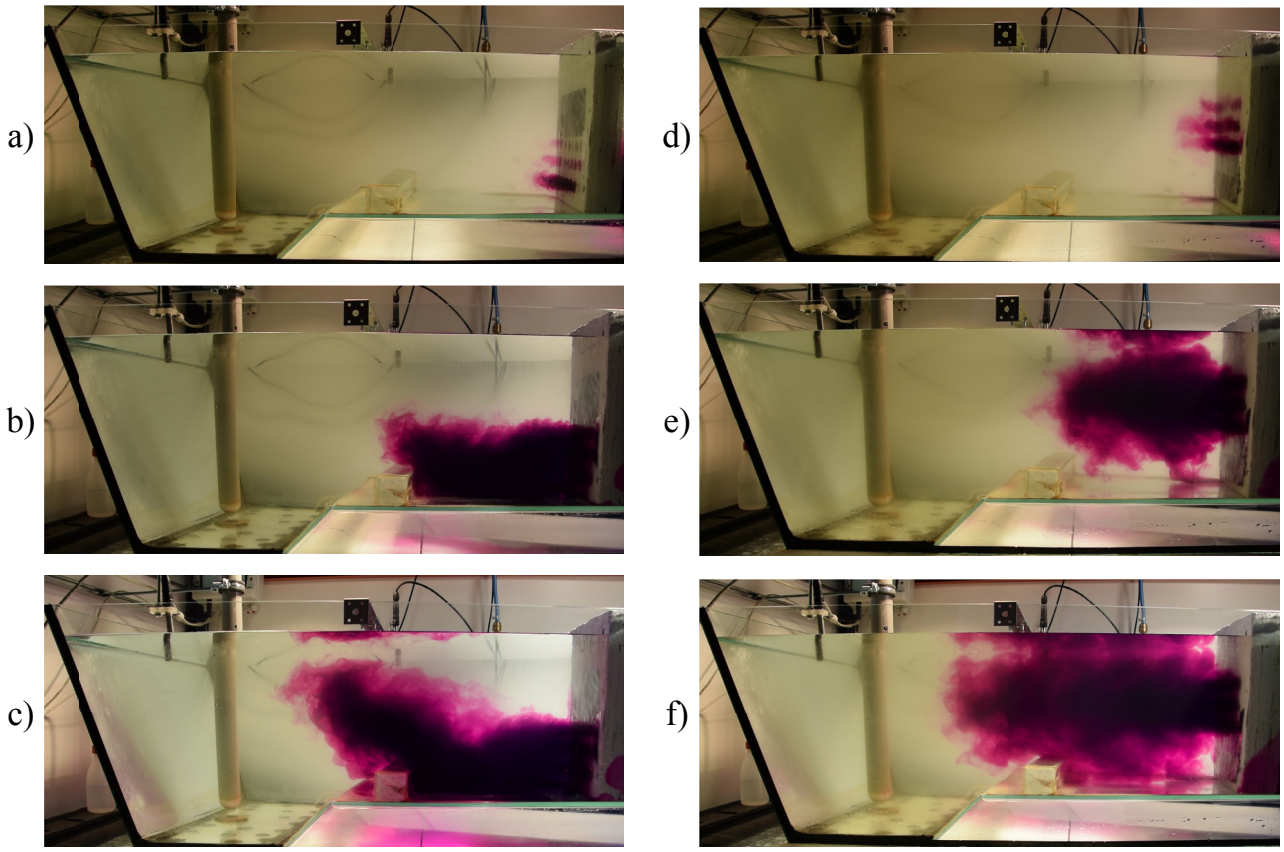

Fig. 2. Behavior of $KMnO_4$ marker in the tundish water model: case 1 – a) after 5s, b) 15s, c) 25s and case 2 – d) 5s, e) 15s, f) 25s

filter than case 1. After 15 seconds, the water main stream in the case 1 is flowing along the tundish bottom. Whereas, in case 2 water main stream towards stopper rod system on the height of filter holes is flowed. After 25 seconds, in case 1 the main stream behind a low dam is directed to the upper surface of the water model. While, the main stream in case 2 isn't changed (comparing with Fig. 2e). The obtained marker structure in both cases are caused by plug flow, which is generated by filter holes. Therefore, the marker is spread on the high of the individual filter hole rows. Only in case 1, direction of the marker flow is changed due to the existing of dam. Furthermore, the non-active zone is noticeable near upper water surface behind filter (in case 1) and along of tundish bottom between dam and filter (in case 2).

4.2. Verification of numerical simulation results

Generated F curves from the numerical simulations in isothermal conditions were compared with measurement points from the water modeling (Fig. 3). In both cases, during the water modeling the measurements points faster achieved dimensionless concentration of next simulated cast steel grade than F curves, which were obtained from numerical simulations. In case 1, only after reaching 0.85 the dimensionless concentration by F curve from the numerical simulation, it is coincided with the measurement points from physical trial no. 5. Whereas, in case 2, after reaching 0.85 the dimensionless concentration by F curve, it coincided with the measurement points from physical trial no. 1 and 2. Figure 4 presents transition zones of both cases from physical trials (average from 6 physical trials), numerical simulations in isothermal and non-isothermal conditions. Despite, the differences in shaping F curves from numerical simulations with the measurement points from water modeling, it can indicate which research case shortens the transition zone, due to the same tendency of the generation transition zone between physical trial and numerical simulations. In both methods case 1 is characterized by a shorter the transition zone than the transition zone from case 2. However, the less differences in the transition zone between cases from numerical simulations (0.07 of dimensionless time) than the transition zone from the physical trials (0.16 of dimensionless time) were observed. Furthermore,

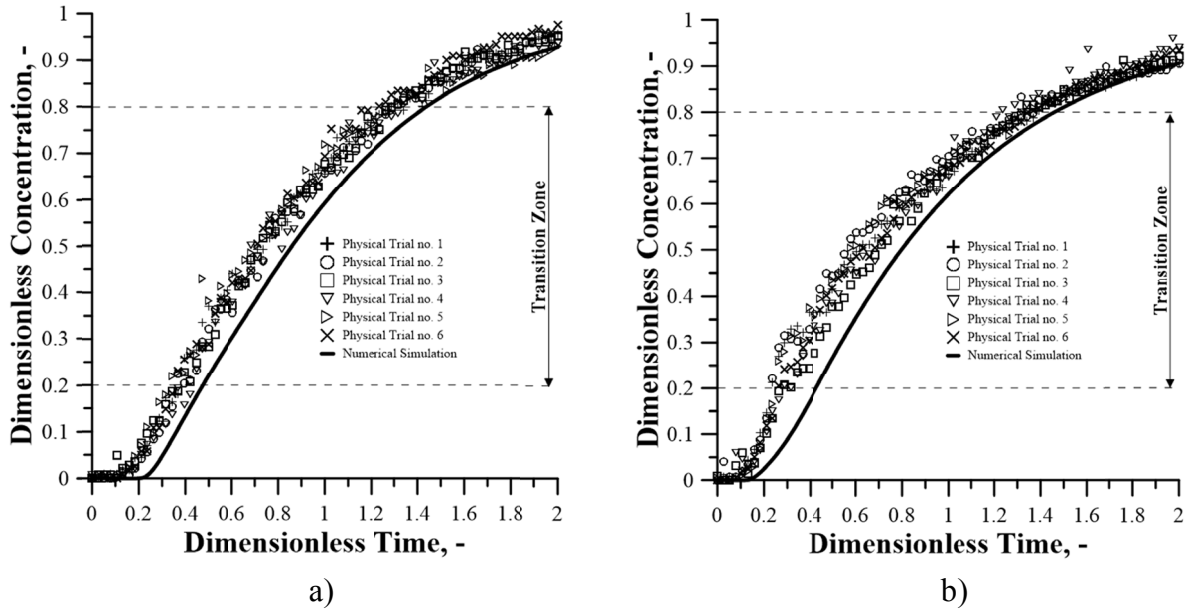

Fig. 3. F curves for isothermal conditions: a) case 1, b) case 2

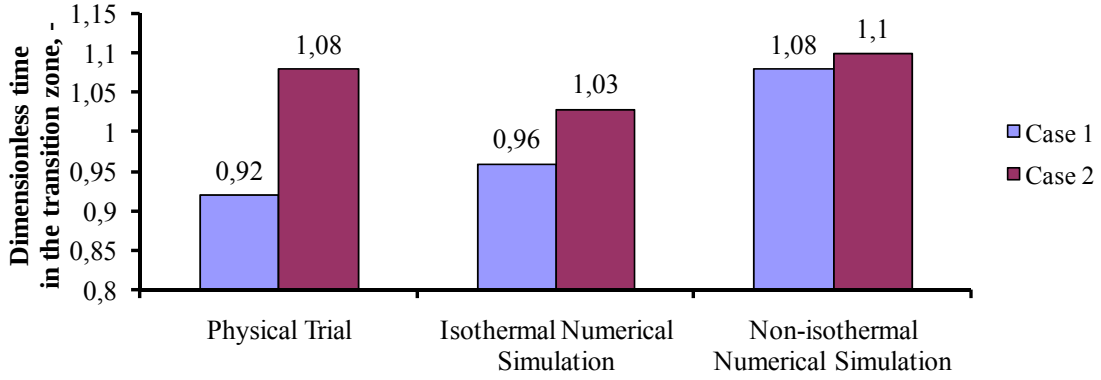

Fig. 4. Transition zone ranges for physical trials and numerical simulations with different thermal conditions

figure 4 presents the transition zone from the numerical simulations in non-isothermal conditions. After taken into account the temperature gradient in the calculations the transition zones were increased and the differences between the transition zones from the both research cases were decreased (0.02 of dimensionless time). Nevertheless, it should be noted that the lower arrangement of holes in the filter has a slight influence on shortening the transition zone during the sequential casting process.

4.3. Liquid steel flow hydrodynamic structure in the tundish

Figure 5 shows the liquid steel flow fields of both cases on a plane passing through the tundish axis. In case 1 and 2 in the zone in front of the multi-hole filter, the liquid steel main stream from ladle shroud is flowed and hit the tundish bottom, after which a vertical circulation stream between the tundish bottom and wall is created. Furthermore, between the multi-hole filter and the tundish bottom a vertical circulation stream is formed. However, the liquid steel flow fields in the zone behind the multi-hole filter more differ between the considered research cases. Analyzing the movement of the liquid steel main stream in the zone behind the multi-hole filter, in both cases it was noted that the liquid steel main stream is directed towards the upper surface of the object. In case 1 and 2, a horizontal circulation stream between the filter wall and the upper surface of the considered object was observed. However, they differ in shape and size. In case 1, a two circulation streams under the upper surface and near the stopper rod system were observed. Also, a circulation stream in the place of lowering the tundish bottom was noticed. In case 2, a wide influence of the horizontal circulation stream from the multi-hole filter to the stopper rod system was noted, to which the backflows from the exit zone of the tundish was reached. Also, the backflows were noted in case 1, which reach behind a dam in front of place of tundish bottom lowering. Generally, in both cases, in front of multi-holes filter the character of liquid steel flow is falling-vertical, whereas behind of multi-holes filter is horizontal. Also, the occurrence of many circulation flows may cause an expansion the non-active flow zone in the tundish. The nature of main stream of liquid steel flow behind the multi-holes filter is advantageous due to the directing of the liquid steel along the liquid steel/ slag interface, which may support in the outflow of non-metallic inclusions into the slag phase.

Figure 6 shows the liquid steel temperature fields of both research cases. In both cases a significant thermal homogenization in the zone in front of the multi-hole filter was noted (in both cases the liquid steel temperature in the filter holes was equal 1822 K). In the tundish zone behind the multi-hole filter, higher temperatures of liquid steel along the upper surface of the object were observed. In case 2, there were significant drops in the liquid steel temperature along the tundish bottom between a dam and the multi-hole filter (1816.5 K). It is caused by the existence of dead zone flow behind the filter and in front of dam. Thus, case 2 is characterized by a slight worse degree of the thermal homogenization in relation to the case 1. At the exit of the tundish in case 1, 1819 K of the liquid steel temperature was noted, whereas 1818.5 K in case 2.

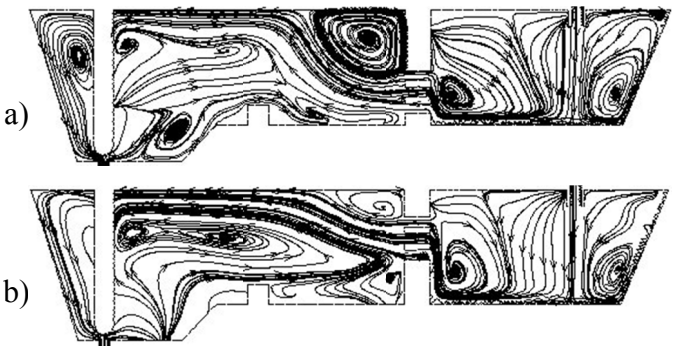

Fig. 5. Liquid steel flow fields in the considered tundish: a) case 1, b) case 2

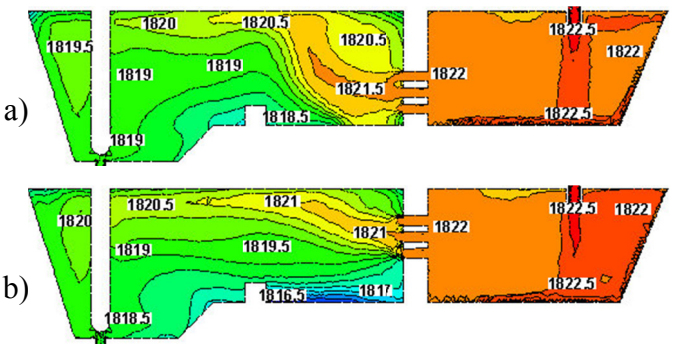

Fig. 6. Liquid steel temperature fields in the considered tundish: a) case 1, b) case 2

4.4. Refining process in the tundish

The next stage of the research was the analysis of non-metallic inclusions behavior in the working volume of the considered tundish. Figure 7 presents the relationship between Al_2O_3 size and quantity of removed non-metallic inclusions from liquid steel. For measurement points, linear regressions were made to better visualize the relationship between Al_2O_3 particle size and quantity of removed non-metallic inclusions. The analysis showed that with the increase of Al_2O_3 particle size its ability to flowing out from liquid steel to the slag in both research cases increase. However, using case 1, a slightly more Al_2O_3 particles from liquid steel were removed in relation to the results using case 2. In case 1, the least of the non-metallic inclusions were removed simulating 10 mm particles (89.46%), whereas the most simulating 50 mm particles (92.78%). In case 2, the least non-metallic inclusions using 5 mm particles (87.6%) were removed and the most using 50 mm particles (90,12%). Figure 8 presents average quantity of removed Al_2O_3 particles from liquid steel, taking into account the locations, where the non-metallic inclusions were assimilated. The quantity of non-metallic inclusions assimilated in the slag layer behind and in front of the multi-hole filter was compared. Furthermore, the

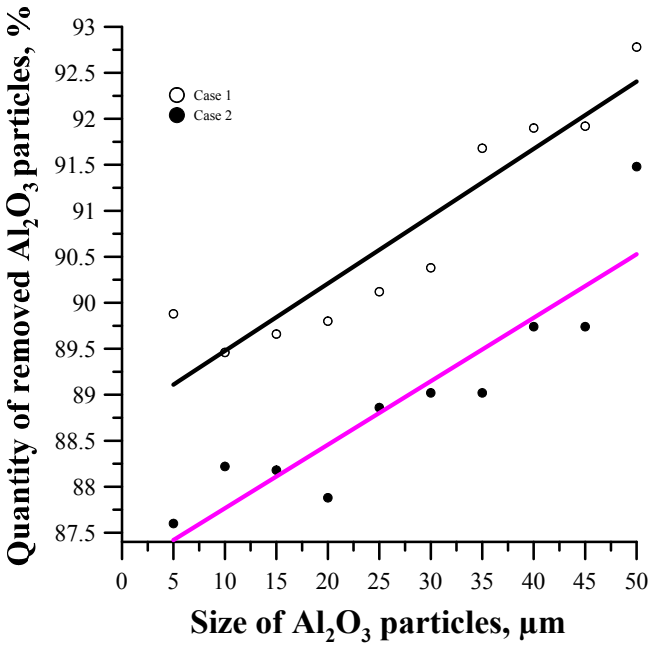

Fig. 7. Quantity of removed Al_2O_3 particles from liquid steel of the considered research cases

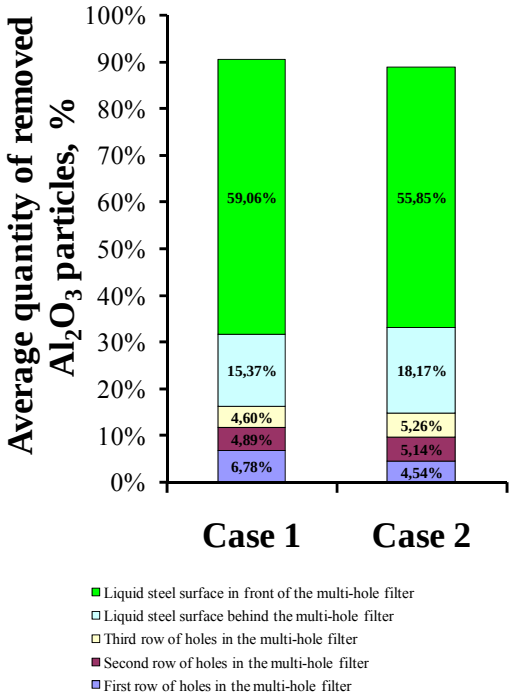

Fig. 8. Average quantity of removed Al_2O_3 particles and its assimilation location in the considered cases

degree of assimilation of non-metallic inclusions in individual rows of holes in the multi-hole filter was checked. In case 1, 90.70% of Al_2O_3 particles from liquid steel were removed, while 88.96% in case 2. In both research cases, most of the Al_2O_3 particles in the slag layer were assimilated (case 1-74,43% and case 2-74,02%). 16.27% of removed non-metallic inclusions in the multi-hole filter in case 1 were assimilated, while 14.94% in case 2. In both cases, a linear tendency of the assimilation Al_2O_3 particles in individual rows of holes in the multi-hole filter was observed (the rows arrangement of holes in the multi-hole filter in table 1 were described). In case 1, the most of the non-metallic inclusions in first row of holes were assimilated (6.78%), but the least of the non-metallic inclusions in third one (4.60%). In case 2, the most Al_2O_3 particles in third row of holes were assimilated (5.26%), while the least in first (4.54%). However, it should be noted that the percentages differences of assimilated Al_2O_3 particles between rows of holes in the multi-hole filter are slight. In addition, in both tested cases, a significant part of non-metallic inclusions flows into the slag phase in front of the multi-hole filter (case 1-59.06% and case 2-55.85%). Therefore, placing the multi-hole filter resulted the generation of the hydrodynamic structure which stimulates to flow out the non-metallic inclusions into the slag in the tundish inlet zone. Figure 9 shows trajectories of the Al_2O_3 particles movement in the considered cases (the individual color of trajectories are assigned to the individual particle). Chaotic motion of Al_2O_3 particles with a size of 5 mm was studied, introducing them into a group of 10 particles. Non-metallic inclusions inflow into the tundish together with the liquid steel, then they bounce off the

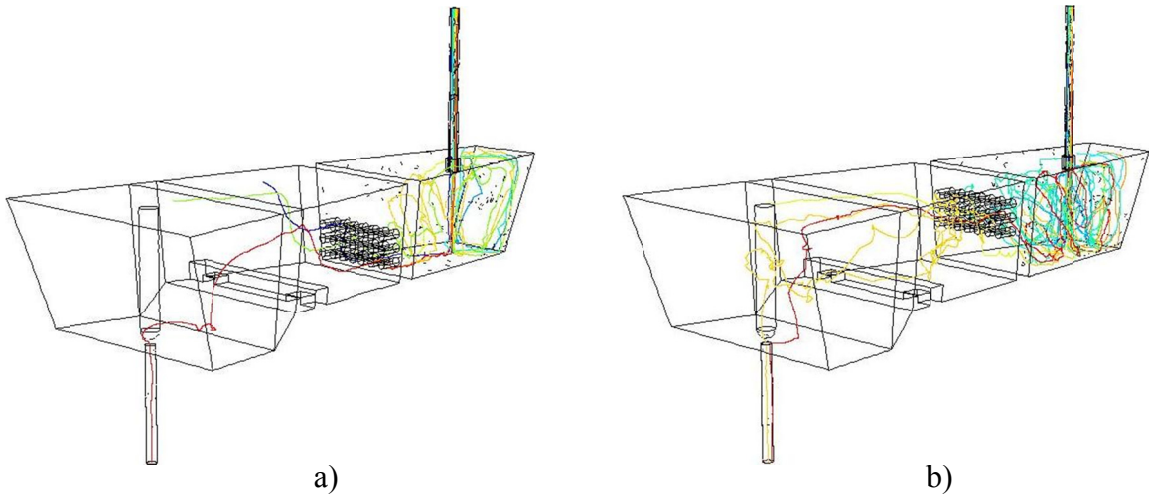

Fig. 9. Trajectories of the Al_2O_3 particles motion in the tundish space: a) case 1, b) case 2

object bottom and next flow along tundish walls towards to the slag phase, where the part of Al_2O_3 particles are assimilated. In tundish zone behind the multi-hole filter in both research cases Al_2O_3 particles towards the upper surface of the object are directed, where the part of non-metallic inclusions in the slag phase are assimilated. The remaining Al_2O_3 particles flow towards the submerged entry nozzle.

5. Summary

The results of numerical simulations supported by the outcomes of water modeling provide a valuable information about the tundish design. In this work, the effect of the arrangement of holes in the multi-hole filter on the hydrodynamic structure and liquid steel refining processes in a tundish was considered. Based on performed examination, it was found that:

- The applied mathematical model in the calculations correlates well with water modeling due to the possibility of determining a research case which was characterized by a shorter the transition zone.
- Both tundish variants give the similar results in the range of the transition zone.
- The main streams of liquid steel flow in both tundish cases behind the multi-hole filter were directed towards the liquid steel/slag interface.
- Both multi-hole filters generate similar thermal homogenization in the internal working tundish volume.
- In both tundish variants, the most quantity of removed Al_2O_3 particles in slag phase in front of the multi-hole filter were assimilated. Whereas, in the multi-hole filter in both variants only about 15% of non-metallic inclusions were assimilated.

Acknowledgements

The research work carried out as part of statutory research of the Department of Metals Extraction and Recirculation, Częstochowa University of Technology.

REFERENCES

[1] A. Tripathi, S.K. Ajmani, ISIJ Int. **51** (10), 1647-1656 (2011).
[2] L. Zhong, B. Li, Y. Zhu, R. Wang, W. Wang, X. Zhang, ISIJ Int. **47** (1), 88-94 (2007).
[3] A. Tripathi, ISIJ Int. **52** (3), 447-456 (2012).
[4] T. Merder, J. Pieprzyca, Steel Res. Int. **83** (11), 1029-1038 (2012).
[5] T. Merder, Arch. Metall. Mater. **58** (4), 1111-1117 (2013).
[6] J. Pieprzyca, T. Merder, M. Saternus, H. Kania, Arch. Metall. Mater. **59** (4), 1433-1440 (2014).
[7] A. Ruckert, M. Warzecha, R. Koitzsch, M. Pawlik, H. Pfeifer, Steel Res. Int. **80** (8), 568-574 (2009).
[8] L. Zhang, S. Tanaguchi, K. Cai, Mater. Trans. **31B** (2), 253-266 (2000).
[9] K. Janiszewski, Metalurgija **52** (1), 71-74 (2013).
[10] K. Uemura, M. Takahashi, S. Koyama, M. Nitta, ISIJ Int. **32** (1), 150-156 (1992).
[11] L. Bulkowski, U. Galisz, H. Kania, Z. Kudliński, J. Pieprzyca, J. Barański, Arch. Metall. Mater. **57** (1), 363-369 (2012).
[12] K. Janiszewski, Arch. Metall. Mater. **58** (2), 513-521 (2013).
[13] K. Janiszewski, B. Panic, Metalurgija **53** (3), 339-342 (2014).
[14] O.B. Isaev, Metallurgist **53** (11-12), 672-678 (2009).
[15] O. Isayev, V. Kislitsa, C. Zhang, K. Wu, A. Hress, Metallurgist **59** (9-10), 980-986 (2016).
[16] A.K. Plappally, M.A.R. Sharif, R.C. Bradt, Fluid Dyn. Mat. Process. **3** (2), 115-128 (2007).
[17] S. Chatterjee, Li D., K. Chattopadhyay, Metall. Mater. Trans. 49B (2), 756-766 (2018).
[18] A. Najera-Bastida, L. Garcia-Demedices, P. Ramirez-Lopez, E. Torres-Alonso, R.D. Morales, Steel Res. Int. **78** (4), 318-326 (2007).
[19] P. Ni, L.T.I. Jonsson, M. Ersson, P.G. Jonsson, Steel Res. Int. **87** (10), 1356-1365 (2016).
[20] V. Singh, A.R. Pal, P. Panigrahi, ISIJ Int. **48** (4), 430-437 (2008).
[21] J. Falkus, J. Lamut, Arch. Metall. Mater. **50** (3), 709-718 (2005).
[22] K. Chattopadyay, M. Hasan, M. Isac, R.I.L. Guthrie, Metall. Mater. Trans. **41B** (1), 225-233 (2010).
[23] J. Huang, Y. Zhang, Y. Zhang, Y. Zhang, X. Ye, B. Wang, Metall. Mater. Trans. **47B** (5), 3144-3157 (2016).
[24] S. Chatterjee, K. Chattopadhyay, Metall. Mater. Trans. **47B** (1), 508-521 (2016).
[25] A. Cwudziński, Steel Res. Int. **81** (2), 123-131 (2010).
[26] A. Cwudziński, Arch. Metall. Mater. **58** (4), 1077-1083 (2013).
[27] M.I.H. Siddiqui, P.K. Jha, ISIJ Int. **53** (11), 2578-2587 (2014).
[28] G. Solorio-Diaz, R.D. Morales, J. Palafox-Ramos, L. Garcia-Demedices, A. Ramos-Banderas, ISIJ Int. **44** (6), 1024-1032 (2004).
[29] A. Cwudziński, Metall. Res. Tech. **111** (1), 45-55 (2014).
[30] R.D. Morales, J.D.J. Barreto, S. Lopez-Ramirez, J. Palafox-Ramos, D. Zacharias, Metall. Mater. Trans. **31B** (6), 1500-1515 (2000).
[31] M. Bielnicki, J. Jowsa, Steel Res. Int. **89** (9), 1800110 (2018).
[32] A. Vargas-Zamora, R.D. Morales, M. Diaz-Cruz, J. Palafox-Ramos, J.D.J. Barreto-Sandoval, Metall. Mater. Trans. **35B** (2), 247-257 (2004).
[33] A. Cwudziński, Steel Res. Int. **85** (5), 902-917 (2013).
[34] Y. Sahai, T. Emi, ISIJ Int. **36** (9), 1166-1173 (1996).
[35] B.G. Thomas, Continuous Casting **10**, 115-127 (2003).
[36] S. Chakraborty, T. Hirose, B. Jones, D.A. Dukelow, Continuous Casting **10**, 41-46 (2003).
[37] A. Cwudziński, Arch. Metall. Mater. **56** (5), 611-618 (2011).
[38] M. Warzecha, T. Merder, P. Warzecha, G. Stradomski, ISIJ Int. **53** (11), 1983-1992 (2013).